COBEM 2023 27TH INTERNATIONAL CONGRESS OF MECHANICAL ENGENEERING

ABCM Brazilian Society of Mechanical Sciences and Engineering
27th ABCM International Congress of Mechanical Engineering
December 04-08, 2023, Florianópolis-SC, Brazil

COB-2023-1693
A VIEW OF THE BEHAVIOUR OF THE SOYBEAN AERATION PROBLEM WITH REALISTIC PARAMETERS

Daniel Rigoni
Graduate Program in Numerical Methods in Engineering, Federal University of Paraná, 81531-980, Curitiba, PR, Brazil
Department of Mathematics, State University of Centro-Oeste, 85040-167, Guarapuava, PR, Brazil
rigoni1@ufpr.br

Marcio Augusto Villela Pinto
Department of Mechanical Engineering, Federal University of Paraná, 81531-980, Curitiba, PR, Brazil
marcio_villela@ufpr.br

Jotair Elio Kwiatkowski Jr.
Department of Computer Science, State University of Centro-Oeste, 85040-167, Guarapuava, PR, Brazil
jotair@unicentro.br

Abstract. *The objective of this study is to present an innovative analytical solution to the mathematical model that characterizes the behaviour of the grain mass aeration process. To achieve this goal, we utilize the Method of Manufactured Solutions (MMS), a well-established method in the field of Computational Fluid Dynamics (CFD) for validating numerical techniques and quantifying their errors. Both the CDS-Crank-Nicolson and Leith techniques were employed using the Finite Difference Method (FDM). An error analysis was performed to evaluate the accuracy of the approximations utilized and to confirm the effective and apparent orders of the discretization error obtained through mesh refinement. Furthermore, the numerical methods were carefully evaluated and compared in two realistic settings of the aeration process of soybeans. The comprehensive study revealed that the Leith approach outperforms the CDS-Crank-Nicolson method in both examined settings. These findings highlight the critical importance of judiciously selecting suitable numerical approximations when tackling complex problems such as grain mass aeration, where variations in the parameters can substantially impact the precision of the final outcomes. The results of this investigation provide valuable insights for researchers and practitioners in the field, offering a basis for informed decision-making and improved problem-solving strategies. Based on these results, it is recommended that Leith's method be used to solve the grain mass aeration model numerically using the FDM due to its exceptional stability, as demonstrated by its superior performance in the two practical settings studied. This can significantly enhance our understanding of the grain mass aeration process and its practical applications in the agricultural industry. By providing a reliable numerical solution, this study offers insight into the optimization of aeration processes, leading to improved grain quality and reduced spoilage. Furthermore, this can have significant implications for the storage and preservation of grains, ensuring their safe and efficient use in various agricultural applications.*

Keywords: *Postharvest, CFD, Thorpe, Finite Difference Method*

1. INTRODUCTION

Global soybean production in 2020 was 337.298 million tons, with Brazil and the United States accounting for 65.68% of this production (FAO, 2020). Soybeans are used in the petroleum and protein industries and require extended storage due to delayed processing (Cañizares et al., 2021).

During the postharvest stage, soybeans maintain an active metabolism. Factors like temperature and moisture content affect their properties, including antioxidant compounds and soybean protein isolate (Ferreira et al., 2019).

Aeration is the most common method for maintaining soybean quality during storage, regulating, and reducing grain mass temperature (Coradi et al., 2020). It is a cost-effective, chemical-free technique for preserving grain quality (Lopes & Neto, 2022).

Accurately predicting the grain storage ecosystem helps develop suitable aeration strategies based on local climate conditions. Temperature and moisture prediction methods are used to assess aeration effectiveness and determine the need for insect, mite, and fungi control. However, testing multiple aeration strategies across seasons in numerous silos can be expensive (El Melki et al., 2022).

Computational Fluid Dynamics (CFD) is a valuable tool that can be employed to simulate and analyse the airflow patterns, temperature distribution, and moisture transfer within grain storage systems (Rigoni et al. 2021, Kwiatkowski Jr. et al. 2022). By applying CFD techniques, researchers can gain insights into the complex dynamics of airflow, identify potential hotspots or areas prone to moisture accumulation, and optimize aeration strategies for enhanced grain quality

and storage efficiency. CFD simulations provide a cost-effective alternative to extensive field testing by allowing for virtual experimentation and evaluation of various aeration scenarios, contributing to a better understanding of the soybean aeration problem (Nuttall et al., 2017).

Rigoni et al. (2022) provided an analytical solution using the method of manufactured solutions (MMS) for Thorpe's (2001) widely used mathematical model of grain mass aeration. The model was numerically solved using the Finite Difference Method (FDM), with the authors recommending the CDS-Crank-Nicolson and Leith's methods.

This paper aims to solve Thorpe's (2001) mathematical model using the FDM and compare the performance of the CDS-Crank-Nicolson and Leith's methods in two different soybean aeration settings. Additionally, the study compares the simulation results with a modified analytical solution that incorporates a broader range of realistic parameters, surpassing the limitations of the previous work presented by Rigoni et al. (2022). This paper also includes an analysis of the discretization error for the utilized approximations to ensure that there are no programming errors in the numerical solution.

To address non-physical oscillations in second-order approximations, the technique by Von Neumann & Richtmyer (1950) was employed, following the approach in Rigoni et al. (2022), Xuan et al. (2017), Mousa & Ma (2020), and Melland et al. (2021).

The paper is structured as follows: Section 2 presents the mathematical model proposed by Thorpe (2001), including the boundary and initial conditions. Section 3 introduces an adapted version of the analytical solution proposed in Rigoni et al. (2022) to incorporate more realistic parameters. The numerical model is described in detail in Section 4. In Section 5, the code is numerically verified. Section 6 presents and discusses the obtained results, while Section 7 draws the conclusions of the study.

2. MATHEMATICAL MODEL

The model that describes the temperature (T) and grain moisture (U) used in this work was presented in detail by Thorpe (2001). However, simplifications have been made to the original model, as suggested by Lopes et al. (2006), to maintain accuracy while improving computational efficiency. The simplified model, adopted in this work, is given by

$$\frac{\partial T}{\partial t}\left(\rho_\sigma\left[c_g + c_W U\right] + \epsilon\rho_a\left[c_a + R\left(c_W + \frac{\partial h_v}{\partial T}\right)\right]\right) =$$
$$\rho_\sigma h_s \frac{\partial U}{\partial t} - u_a\rho_a\left[c_a + R\left(c_W + \frac{\partial h_v}{\partial T}\right)\right]\frac{\partial T}{\partial y} + \rho_\sigma \frac{dm}{dt}(Q_r - 0.6h_v), \quad (1)$$

$$\rho_\sigma \frac{\partial U}{\partial t} = -u_a\rho_a \frac{\partial R}{\partial y} + \frac{dm}{dt}(0.6 + U), \quad (2)$$

where: t is time (s), y is the axis in the vertical direction (oriented from bottom to top) (m), U is grain moisture ($\mathrm{kgkg^{-1}}$), u_a is aeration air velocity ($\mathrm{ms^{-1}}$), c_g is grain specific heat ($\mathrm{Jkg^{-1}{}^\circ C^{-1}}$), c_W is specific heat of water ($\mathrm{Jkg^{-1}{}^\circ C^{-1}}$), c_a is specific heat of air ($\mathrm{Jkg^{-1}{}^\circ C^{-1}}$), R is humidity ratio of air ($\mathrm{kgkg^{-1}}$), ρ_a is density of intergranular air ($\mathrm{kgm^{-3}}$), ρ_σ is grain bulk density ($\mathrm{kgm^{-3}}$), h_v is latent heat of vaporization of water ($\mathrm{Jkg^{-1}}$), h_s is differential heat of sorption ($\mathrm{Jkg^{-1}}$), T is grain temperature (°C), ϵ is grain porosity (decimal), dm/dt is derivative of the grain dry matter loss with respect to time ($\mathrm{kgs^{-1}}$) and Q_r is heat of oxidation of the grain ($\mathrm{Js^{-1}m^{-3}}$).

In this study, an aeration system with an up-flow configuration, represented by the vertical dimension $y \in [0, L]$, was utilized. The problem geometry and calculation domain for this study are depicted in Figure 1. The domain is a three-dimensional silo, representing the storage structure used for soybean grains. The vertical dimension, denoted by y, ranges from 0 to L, representing the height of the grain mass. The horizontal dimensions, denoted by x and z, extend in the plane perpendicular to the vertical dimension. However, for the purpose of this study, a one-dimensional simplification is adopted, focusing solely on the vertical dimension ($y \in [0, L]$). This simplification allows for easier analysis and computational implementation while still capturing the essential aspects of the aeration system.

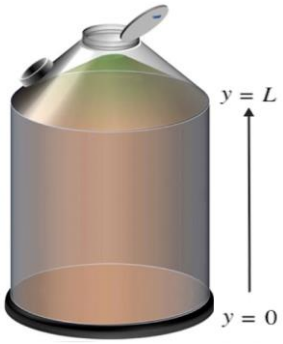

Figure 1. Problem geometry and calculation domain (Modified from Panigrahi et al. (2020b)).

The parameters of the mathematical model were specifically derived for soybean grains, and the equations employed in the analysis align with the detailed formulations presented by Rigoni et al. (2022). By utilizing these consistent equations and accurate parameter values, the study ensures a robust and reliable foundation for investigating the behaviour of the soybean aeration problem.

2.1 Boundary and Initial Conditions

At $y = 0$, it was assumed that the grain at the base of the storage reaches equilibrium with the aeration airflow:

$$T(0,t) = T_B, \tag{3}$$

where T_B represents the aeration air temperature. The moisture content at $y = 0$ was calculated as (Lopes et al. 2006)

$$U(0,t) = -\frac{1}{B} ln\left[ln\left(-\frac{r_a}{100}\right)\left(-\frac{T_B + C}{A}\right)\right] = U_B, \tag{4}$$

where r_a represents the relative humidity of the aeration airflow and can be obtained by

$$r_a = u_r \frac{\frac{6 \times 10^{25}}{(T_{amb} + 273.15)^5} exp\left[-\frac{6800}{T_{amb} + 273.15}\right]}{\frac{6 \times 10^{25}}{(T_B + 273.15)^5} exp\left[-\frac{6800}{T_B + 273.15}\right]}, \tag{5}$$

where u_r is the ambient relative humidity and T_{amb} is the ambient temperature. At $y = L$, the Neumann boundary conditions for temperature and moisture are given by

$$\left(\frac{\partial T}{\partial y}\right)_{y=L} = \left(\frac{\partial U}{\partial y}\right)_{y=L} = 0. \tag{6}$$

Throughout the domain, the initial condition is equal to the temperature of the grain mass after the drying process (T_I), that is:

$$T(y,0) = T_I. \tag{7}$$

The initial moisture (U_I) can be obtained by (Thorpe, 2001b)

$$U(y,0) = \frac{U_p}{100 - U_p} = U_I, \tag{8}$$

where U_p is the moisture content of the grain after drying, in percent (%).

3. ANALYTICAL SOLUTION

The Method of Manufactured Solutions (MMS) (Oberkampf & Blottner, 1998) involves generating an exact solution without concerning the physical reality of the problem. An analytic function is defined as the dependent variable in the partial differential equation (PDE), and all derivatives are computed analytically. The remaining terms that do not satisfy the PDE are incorporated into a source term, which is added to the PDE to precisely satisfy the new equation (Roy, 2005).

Rigoni et al. (2022) were the first to propose an analytical solution to the model introduced by Thorpe (2001). Their solution was developed using the MMS approach based on experimental data from Khatchatourian & Oliveira (2006) and Oliveira et al. (2007). The experiment involved monitoring the temperature of soybeans in a prototype silo, with the aeration process being observed for a duration of one hour. The initial grain temperature (T_I) was 52.9 °C, and the aeration air temperature (T_B) was 31.1 °C.

Although the analytical solution proposed by Rigoni et al. (2022) demonstrated excellent agreement with the experimental data, it did not consider the initial parameter of aeration air velocity. To address this limitation, the solution was algebraically manipulated, leading to the proposal of a new analytical solution that incorporates this parameter. Therefore, the new analytical solution presented in this paper is given by:

$$\hat{T}(y,t) = T_I + \frac{1}{2}(T_B - T_I)[erfc(P_1) + exp(P_2)erfc(P_3)], \tag{9}$$

where $P_1 = \frac{y-u_a\frac{2.2\times10^{-4}}{0.23}t}{\sqrt{u_a\frac{8\times10^{-6}}{0.23}t}}$, $P_2 = \frac{u_a\frac{2.2\times10^{-4}}{0.23}y}{u_a\frac{8\times10^{-6}}{0.23}}$, $P_3 = \frac{y+u_a\frac{2.2\times10^{-4}}{0.23}t}{\sqrt{u_a\frac{8\times10^{-6}}{0.23}t}}$ and *erfc* represents the complementary error function (Van Genuchten et al., 1982), defined by

$$erfc(x) = 1 - erf(x) = \frac{2}{\sqrt{\pi}}\int_x^{\infty} e^{-t^2}\,dt. \tag{10}$$

The proposed solution considers the following parameters: storage size (y), aeration time (t), aeration air temperature (T_B), initial grain mass temperature (T_I), and aeration air velocity (u_a).

These parameters play a crucial role in analysing the behaviour of numerical solutions when variations occur. By modifying these parameters, it becomes possible to study the impact of temperature, aeration time, aeration air temperature, initial grain mass temperature and aeration air velocity on the numerical solution. This comparative analysis is essential for assessing the sensitivity of the solution to parameter changes and understanding how different parameter values affect the overall behaviour of the system. It helps in validating the accuracy and reliability of the numerical solutions and provides valuable insights into the system's response under various conditions.

For the function defined by Eq. (9) to be considered an analytical solution of Eq. (1), a source term needs to be added to Eq. (1), resulting in the following modified equation:

$$\mathcal{A}\frac{\partial T}{\partial t} = -\mathcal{B}\frac{\partial T}{\partial y} + \mathcal{F}, \tag{11}$$

where:

$$\mathcal{A} = \rho_\sigma\left[c_g + c_W U\right] + \epsilon\rho_a\left[c_a + R\left(c_W + \frac{\partial h_v}{\partial T}\right)\right], \tag{12}$$

$$\mathcal{B} = u_a\rho_a\left[c_a + R\left(c_W + \frac{\partial h_v}{\partial T}\right)\right], \tag{13}$$

$$\mathcal{F} = \mathcal{A}\left(\frac{\mathcal{F}_1}{2}(T_B - T_I)\right) + \mathcal{B}\left(\frac{\mathcal{F}_2}{2}(T_B - T_I)\right), \tag{14}$$

and,

$$\mathcal{F}_1 = \frac{1}{(tu_a)^{\frac{3}{2}}}0.0457519u_a(T_B - T_I)\,exp\left(-\frac{28.750y^2}{tu_a} - 0.0263043tu_a - 27.5y\right)\{y[1045.45 + 1045.45\,exp(82.5y)] + + tu_a(exp(82.5y) - 1)\},$$

$$\mathcal{F}_2 = 27.5\,exp(27.5y)\,erfc\left(\frac{169.558(0.000956522tu_a+y)}{\sqrt{tu_a}}\right) + \frac{1}{\sqrt{tu_a}}\left(-191.326\,exp\left(-\frac{28.75y^2}{tu_a}\right) + - 0.026043tu_a - 27.5y\right) - 191.326\,exp\left[-\left(\frac{28750(y-0.000956522tu_a)^2}{tu_a}\right)\right].$$

4. NUMERICAL MODEL

The grain temperature and moisture differential equations were numerically solved using the Finite Difference Method (FDM) (Tannehill et al., 1997). When an equation is discretized using this method, the evaluation of variables and approximations of their derivatives at the mesh nodes leads to a system of equations that requires a suitable solver. In this study, the TriDiagonal Matrix Algorithm (TDMA) (Thomas, 1949), a widely adopted solver in the literature, was employed to solve the resulting system of equations.

In Figure 2, the position of discrete points relative to a central node *P* is denoted by *N* and *S*. The temporal location of the node is indicated by the subscript *n*. Additionally, $\Delta y = L/N_y$ represents the spacing between two consecutive nodes in the *y* direction, where N_y is the total number of nodes. Similarly, $\Delta t = t_f/N_t$ represents the difference between the current and previous simulation time, where t_f is the final simulation time and N_t corresponds to the number of time steps. These definitions are essential for understanding the discretization and temporal aspects of the numerical solution.

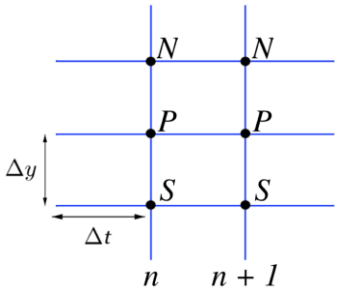

Figure 2. Mesh for the numerical solution using the Finite Difference Method (FDM), involving the central node *P* and its neighbours at two different time steps.

4.1 Central Difference Scheme (CDS)

Approximating the spatial derivative of *T* using CDS and the temporal derivative of *T* using the θ-formulation (Tannehill et al., 1997), the discretized form of Eq. (11) is given by

$$\mathcal{A}^{\theta}T_P^{n+1} = \mathcal{A}^{\theta}T_P^{n} - \frac{\mathcal{B}^{\theta}}{2}\left(\frac{\Delta t}{\Delta y}\right)T_E^{\theta} + \frac{\mathcal{B}^{\theta}}{2}\left(\frac{\Delta t}{\Delta y}\right)T_W^{\theta} + \mathcal{F}\Delta t, \tag{15}$$

where,

$$\mathcal{A}^{\theta} = \rho_{\sigma}\left[c_g + c_W U_P^{\theta}\right] + \epsilon\rho_a\left[c_a + R_P^{\theta}\left(c_W + \frac{\partial h_v}{\partial T}\right)\right], \tag{16}$$

$$\mathcal{B}^{\theta} = u_a\rho_a\left[c_a + R_P^{\theta}\left(c_W + \frac{\partial h_v}{\partial T}\right)\right]. \tag{17}$$

Using the same approximations for *U* and *R*, the discretized form of Eq. (2) is obtained:

$$U_P^{n+1} = U_P^{n} - \frac{u_a\rho_a}{2\rho_{\sigma}}\left(\frac{\Delta t}{\Delta y}\right)R_E^{\theta} + \frac{u_a\rho_a}{2\rho_{\sigma}}\left(\frac{\Delta t}{\Delta y}\right)R_W^{\theta} + \frac{\Delta t\frac{dm}{dt}}{\rho_{\sigma}}U_P^{\theta} + 0.6\frac{\Delta t\frac{dm}{dt}}{\rho_{\sigma}}, \tag{18}$$

in which the relation for an arbitrary variable Λ is given by

$$\Lambda^{\theta} = \Lambda^{n} + \theta(\Lambda^{n+1} - \Lambda^{n}). \tag{19}$$

The Neumann boundary conditions can be approximated using CDS with the ghost point technique (Tannehill et al., 1997), so the temperature *T* and the moisture *U* at $y = L$ can be calculated, respectively, by

$$T_{N_B}^{n+1} = T_{N_B}^{n} + \mathcal{F}\frac{\Delta t}{\mathcal{A}}, \tag{20}$$

$$U_{N_B}^{n+1} = U_{N_B}^{n} + \frac{\Delta t\frac{dm}{dt}}{\rho_{\sigma}}U_P^{\theta} + 0.6\frac{\Delta t\frac{dm}{dt}}{\rho_{\sigma}}, \tag{21}$$

where N_B represents the node located at the boundary.

4.2 Leith's Scheme

Equation (11) can be rewritten as

$$\frac{\partial T}{\partial t} = -\left(\frac{\mathcal{B}}{\mathcal{A}}\right)\frac{\partial T}{\partial y} + \frac{\mathcal{F}}{\mathcal{A}}. \tag{22}$$

Leith's scheme (Leith, 1965) consists in approximating the temporal and spatial derivatives of a given variable, in this case *T*, as follows:

$$\left(\frac{\partial T}{\partial t}\right)_P^{n+1} \approx \left[\frac{T_P^{n+1} - T_P^{n}}{\Delta t}\right], \tag{23}$$

$$\left(\frac{\partial T}{\partial y}\right)_P^{n+1} \approx \left(\frac{\mathcal{B}}{\mathcal{A}}\right)\left(\frac{\Delta t}{\Delta y}\right)\left[\frac{T_P^n - T_W^n}{\Delta y}\right] + \left[1 - \left(\frac{\mathcal{B}}{\mathcal{A}}\right)\left(\frac{\Delta t}{\Delta y}\right)\right]\left[\frac{T_E^n - T_W^n}{2\Delta y}\right]. \tag{24}$$

Thus, the discretized form of Eq. (22) is achieved:

$$T_P^{n+1} = \left[1 - \left(\frac{\mathcal{B}}{\mathcal{A}}\frac{\Delta t}{\Delta y}\right)^2\right] T_P^n + \frac{1}{2}\left[\left(\frac{\mathcal{B}}{\mathcal{A}}\frac{\Delta t}{\Delta y}\right)^2 + \left(\frac{\mathcal{B}}{\mathcal{A}}\frac{\Delta t}{\Delta y}\right)\right] T_W^n + \frac{1}{2}\left[\left(\frac{\mathcal{B}}{\mathcal{A}}\frac{\Delta t}{\Delta y}\right)^2 - \left(\frac{\mathcal{B}}{\mathcal{A}}\frac{\Delta t}{\Delta y}\right)\right] T_E^n + \mathcal{F}\frac{\Delta t}{\mathcal{A}}. \tag{25}$$

The same procedure can be done in Eq. (2), resulting in the discretized form, given by

$$U_P^{n+1} = \left[\frac{2\rho_\sigma}{2\rho_\sigma - \frac{dm}{dt}\Delta t}\right](\mathcal{U}_1 + \mathcal{U}_2), \tag{26}$$

where

$$\mathcal{U}_1 = \left(1 + \frac{\frac{dm}{dt}\Delta t}{2\rho_\sigma}\right) U_P^n - \left(\frac{u_a\rho_a}{\rho_\sigma}\frac{\Delta t}{\Delta y}\right)^2 R_P^n + \frac{1}{2}\left[\left(\frac{u_a\rho_a}{\rho_\sigma}\frac{\Delta t}{\Delta y}\right)^2 + \left(\frac{u_a\rho_a}{\rho_\sigma}\frac{\Delta t}{\Delta y}\right)\right] R_W^n,$$

$$\mathcal{U}_2 = +\frac{1}{2}\left[\left(\frac{u_a\rho_a}{\rho_\sigma}\frac{\Delta t}{\Delta y}\right)^2 - \left(\frac{u_a\rho_a}{\rho_\sigma}\frac{\Delta t}{\Delta y}\right)\right] R_E^n + \frac{0.6\Delta t\frac{dm}{dt}}{\rho_\sigma}.$$

Neumann boundary conditions can be approximated using the ghost point technique (Tannehill et al., 1997), whose results are analogous to Eqs. (20) and (21).

4.3 Artificial Viscosity

Originally introduced by Von Neumann & Richtmyer (1950), the artificial viscosity is a method to control spurious non-physical oscillations in numerical solutions and can be added to the temperature equation. Thus, Eq. (11) can be rewritten as

$$\mathcal{A}\frac{\partial T}{\partial t} = -\mathcal{B}\frac{\partial T}{\partial y} + \frac{\partial}{\partial y}\left[D\Delta y^2\left|\frac{\partial T}{\partial y}\right|\frac{\partial T}{\partial y}\right] + \mathcal{F}, \tag{27}$$

where D is a dimensionless constant (Campbell & Vignjevic, 2009). Note that, as $\Delta y \to 0$, the term corresponding to the artificial viscosity tends to zero. Therefore, Eq. (27) tends to Eq. (11).

The method presented by Lax & Wendroff (1960) was used to perform the discretization. For the problem in this study, the artificial viscosity was used to eliminate excessive oscillations in the second-order methods. In this regard, it is appropriate to add the following term in the discretized equations of these methods:

$$\frac{\partial}{\partial y}\left[D\Delta y^2\left|\frac{\partial T}{\partial y}\right|\frac{\partial T}{\partial y}\right] \approx \frac{D}{\Delta y}[|T_E^n - T_P^n|(T_E^n - T_P^n) - |T_P^n - T_W^n|(T_P^n - T_W^n)]. \tag{28}$$

5. NUMERICAL VERIFICATION

This section provides a comprehensive analysis of the code, ensuring accuracy and reliability of the results. To assess the accuracy of the numerical model, the effective (p_E) and the apparent order (p_U) were calculated. These orders estimate the asymptotic order of the discretization error. The p_E is determined when the analytical solution is known, while the p_U is used when the analytical solution is unknown. Both orders are calculated using numerical solutions and representative mesh sizes (h).

The asymptotic order (p_L) for the CDS-Crank-Nicolson and Leith methods used in this study is $p_L = 2$. This information is based on previous studies by Dehghan (2005), Campbell & Yin (2007), and Tannehill et al. (1997). The asymptotic order indicates the expected behaviour of the error as the mesh size tends to zero.

Results related to the discretization errors, p_E and p_U for temperature T at $y = L/2$ and $t = t_f/2$ are presented for the approximations used. The representative mesh size h was calculated as $h = \Delta y = \Delta t/2$ in the tests. The behaviours of the discretization errors with mesh refinement for the methods used are shown in Figure 3.

It can be observed that the discretization error decreased as the mesh size was refined for both methods studied (CDS-Crank-Nicolson and Leith). Furthermore, the curves have similar slopes, suggesting that these errors fall within the same order.

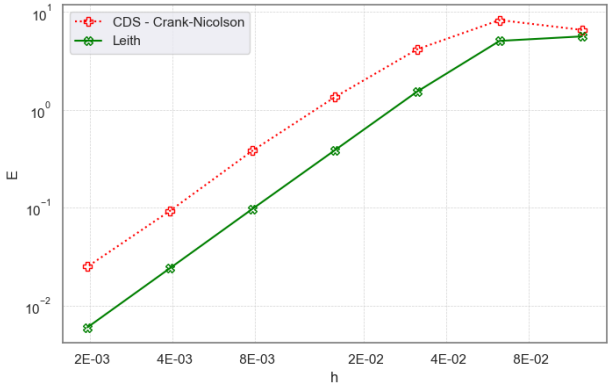

Figure 3: Decay of discretization errors with mesh refinement.

Figure 4 presents the effective (p_E) and apparent (p_U) orders with mesh refinement for each of the methods under study. These orders provide insights into the convergence behavior of the numerical solutions.

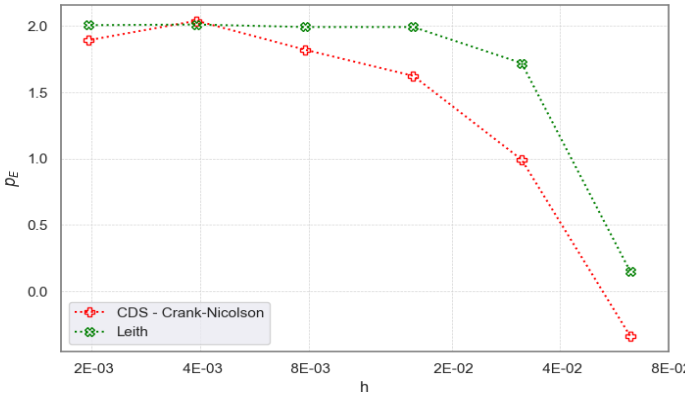

Figure 4.1: Effective Order

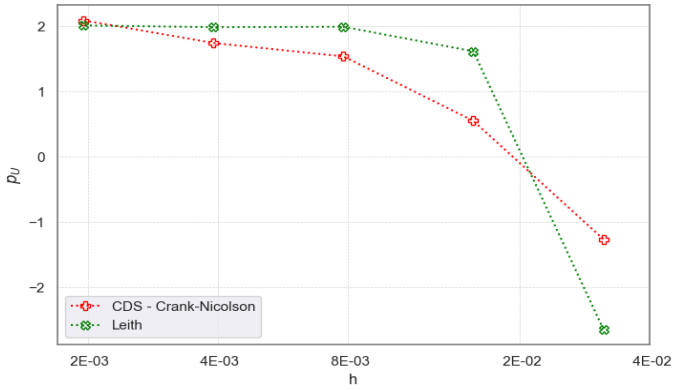

Figure 4.2: Apparent Order

Figure 4: Behaviour of the effective and apparent orders of discretization errors with mesh refinement for the methods under study.

In Figure 4, it is evident that the p_E and p_U of each method converge towards their asymptotic orders (p_L). This convergence supports the reliability and accuracy of the numerical results obtained in the study.

6. NUMERICAL EXPERIMENTS AND RESULTS

Simulations were conducted using various grid sizes, including N_y x N_t = 512x1024, 256x1024, 128x1024, 64x1024, and 32x1024, to examine the performance of the CDS-Crank-Nicolson and Leith's methods in two distinct aeration settings. In the subsequent sections, the performance of the CDS-Crank-Nicolson and Leith's methods will be discussed for all the mesh sizes considered. However, the specific results and figures will be presented for the 512x1024 mesh size as an illustrative example. This approach allows for a comprehensive analysis of the methods across different mesh sizes while highlighting the trends and patterns observed in the selected 512x1024 case.

6.1 Setting A

For the initial setting, referred to as setting A, a soybean mass with a height of 20 meters (L = 20 m) was considered. The initial and boundary temperatures were set to T_I = 52.9 °C and T_B = 31.1 °C, respectively. A constant aeration air velocity of u_a = 0.10 m/s was applied for a duration of 40 hours. Figure 5 illustrates the temperature variation of the soybeans during aeration, specifically focusing on the middle of the storage location (L_m = 10 m). Figure 5.1 depicts the temporal variation of the temperature, while Figure 5.2 shows the numerical error between the computed and analytical temperature for each analysed point in Figure 5.1.

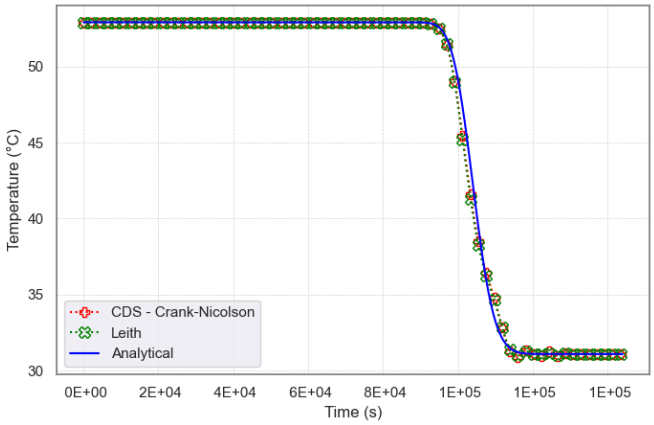

Figure 5.1: Temperature variation with respect to time for L_m= 10 *m*.

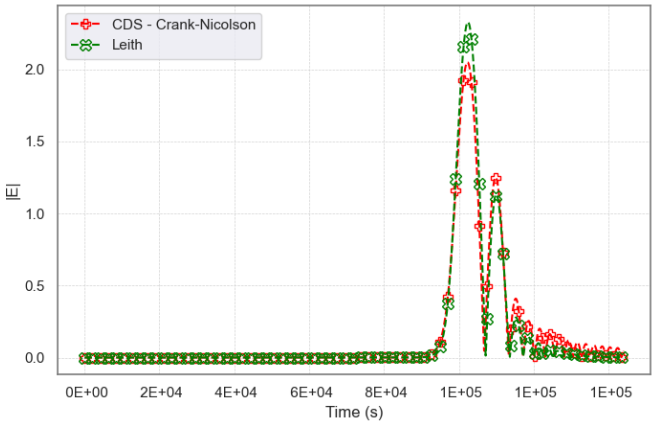

Figure 5.2: Numerical error of temperature *versus* time given by Figure 5.1.

Figure 5: Grain temperature variations in setting A with $N_y x N_t$ = 512x1024.

By utilizing a mesh size of 512x1024, we analysed the performance of the CDS-Crank-Nicolson and Leith's methods in setting A. Figure 5 presents the grain temperature variations for this mesh size. In this case, the CDS-Crank-Nicolson method exhibited better performance compared to the Leith's method. This is evident from the slightly smaller maximum numerical errors observed in Figure 5.2 when using the CDS-Crank-Nicolson method.

In the tests carried out with the other meshes, it could be seen that the difference between the number of time steps (N_t) and the number of spatial points (N_y) plays a crucial role in the accuracy of the numerical solutions. During that test, it was observed that when the difference between N_y and N_t is large, the CDS-Crank-Nicolson and Leith's methods exhibit the same behaviour. With a smaller difference between N_y and N_t (512x1024), the CDS-Crank-Nicolson method was able to provide more precise results.

6.2 Setting B

The second setting referred to as setting B, encompasses a larger storage location with a height of 35 meters (L = 35 m). In line with setting A, the initial and boundary temperatures remain identical. However, in setting B, a higher constant aeration air velocity of u_a = 0.20 m/s is implemented for a duration of 40 hours. It is important to note that setting B features a larger storage area and a more robust fan/motor system compared to setting A.

For comparison purposes, Figure 6 illustrates the temperature variation of soybeans during aeration. Figure 6.1 displays the temporal variation of grain temperature at the midpoint of the storage location (L_m = 17.5 m). The numerical error, represented by the difference between the numerical and analytical temperature, is shown for each analysed point in Figure 6.2.

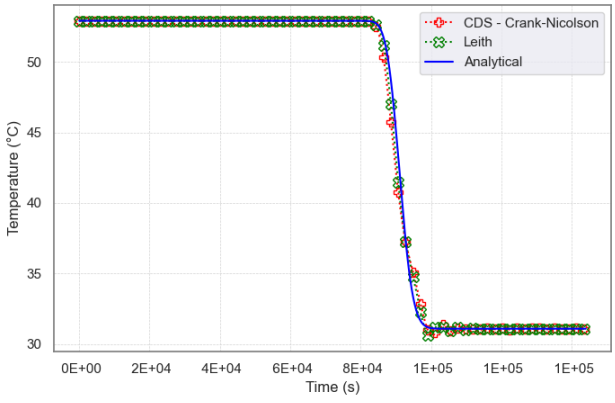

Figure 6.1: Temperature variation with respect to time for L_m = 17.5 *m*.

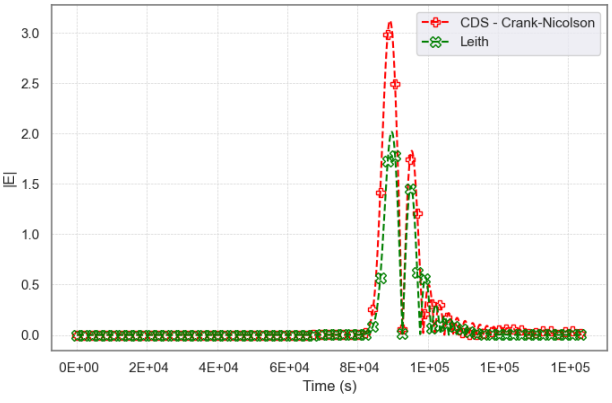

Figure 6.2: Numerical error of temperature *versus* time given by Figure 6.1.

Figure 6: Grain temperature variations in setting B with $N_y x N_t$ = 512x1024.

In setting B, when the difference between N_y and N_t is large, the methods tend to have similar behavior, with a slight advantage for the Leith's method. However, when we consider N_y x $N_t = 512$x1014, as shown in Figure 6, it is evident that the Leith's method is vastly superior to the CDS-Crank-Nicolson method. The numerical errors are significantly smaller for the Leith's method (Figure 6.2), indicating its higher accuracy and reliability in capturing the behavior of the aeration process.

6.3 Discussions

In setting A, characterized by smaller storage locations and lower aeration air velocities, the CDS-Crank-Nicolson method exhibited a consistent and satisfactory performance regardless of the difference between the N_y and N_t parameters, however, the Leith's method showed similar behaviour. In contrast, in setting B, which involved larger storage locations and higher aeration air velocities, the Leith's method consistently outperformed the CDS-Crank-Nicolson method in all tested cases, including those with smaller differences between N_y and N_t.

The robustness, efficiency, and stability demonstrated by the Leith's method, even in cases with smaller differences between N_y and N_t, make it a preferred choice for simulating aeration in grain storage systems. This indicates that the Leith's method can generate accurate and reliable results even when there are variations or uncertainties in the input parameters or conditions. On the other hand, the CDS-Crank-Nicolson method may be more sensitive to changes in the input parameters, potentially rendering it less reliable in certain situations.

In summary, the Leith's method offers robustness and efficiency, making it the preferred option for simulating aeration in grain storage systems, particularly in settings with larger storage locations and higher aeration air velocities. Its ability to handle smaller differences between N_y and N_t further enhances its reliability and applicability in practical settings.

7. CONCLUSIONS

This paper presents a novel analytical solution utilizing the Method of Manufactured Solutions (MMS) based on the work of Rigoni et al. (2022) for the mathematical model of grain mass aeration originally developed by Thorpe (2001). The proposed solution is versatile and capable of handling various parameters associated with soybean aeration. The Finite Difference Method (FDM) was employed to discretize the mathematical model, and particular attention was given to investigating the behaviour of the CDS-Crank-Nicolson and Leith's methods regarding their performance in different settings. To mitigate non-physical oscillations, artificial viscosity was introduced to the problem. Simulations were conducted in various aeration settings, considering different parameters. The findings revealed that the Leith's method exhibited superior efficiency and robustness compared to the CDS-Crank-Nicolson method. As a result, the Leith's method is highly recommended for numerical solutions of the mathematical model pertaining to the aeration problem proposed by Thorpe.

8. REFERENCES

Campbell, L. J., & Yin, B. (2007). On the stability of alternating-direction explicit methods for advection-diffusion equations. Numerical Methods for Partial Differential Equations: An International Journal, 23, 1429–1444. doi:doi/10.1002/num.20233

Cañizares, L. d., Timm, N. d., Lang, G. H., Gaioso, C. A., Ferreira, C. D., & Oliveira, M. d. (2021). Effects of using wind exhausters on the quality and cost of soybean storage on a real scale. Journal of Stored Products Research, 93, 101834. doi:https://doi.org/10.1016/j.jspr.2021.101834.

Coradi, P., Oliveira, M., O. C., Souza, G., Elias, M., & Brackmann, A. (2020). Technological and sustainable strategies for reducing losses and maintaining the quality of soybean grains in real production scale storage units. Journal of Stored Products Research, 87, 101624. doi:https://doi.org/10.1016/j.jspr.2020.101624

Dehghan, M. (2005). Quasi-implicit and two-level explicit finite-difference procedures for solving the one-dimensional advection equation. Applied mathematics and computation, 167, 46–67. doi:10.1016/j.amc.2004.06.067

El Melki, M. N., El Moueddeb, K., & Beyaz, A. (2022). Cooling Potential of Bin Stored Wheat by Summer and Autumn Aeration. Journal of Agricultural Sciences, 28(1), 145 - 158. doi:https://doi.org/10.15832/ankutbd.715508

FAO. (2020). Food and Agriculture Organization of the United Nations. Fonte: http://www.fao.org/publications/sofa/en/

Ferreira, C., Ziegler, V., Goebel, J., Hoffmann, J., Carvalho, I., & Chaves, F. (2019). Changes in phenolic acids and isoflavone contents during soybean drying and storage. Journal of Agricultural and Food Chemistry, 67(4), 1146–1155. doi:https://doi.org/10.1021/acs.jafc.8b06808

Khatchatourian, O. A., & Oliveira, F. A. (2006). Mathematical modeling of airflow and thermal state in large aerated grain storage. Biosystems Engineering, 95, 159–169. doi:10.1016/j.biosystemseng.2006.05.009

Kwiatkowski Jr., J. E. Araki L. K., Pinto, M. A. & Rigoni, D. (2022). Modelising the grain mass aeration process using the Thorpe Model with the Finite Volume Method. Proceedings of the XLIII Ibero-Latin-American Congress on Computational Methods in Engineering, ABMEC.

Lax, P., & Wendroff, B. (1960). Systems of conservation laws. Communications on Pure and Applied Mathematics, 13, 217.

Leith, C. E. (1965). Numerical simulation of the earth's atmosphere. Methods Computational Physics, 4, 1–28.

Lopes, D. C., Martins, J. H., Melo, E. C., & Monteiro, P. M. (2006). Aeration simulation of stored grain under variable air ambient conditions. Postharvest Biology and Technology, 42, 115–120. doi:10.1016/j.postharvbio.2006.05.007

Lopes, D., & Neto, A. J. (2022). Zephyrus: Grain Aeration Strategy Based on the Prediction of Temperature and Moisture Fronts. Em Information and Communication Technologies for Agriculture—Theme III: Decision (Vol. 184). Springer Optimization and Its Applications. doi:https://doi.org/10.1007/978-3-030-84152-2_9

Melland, P., Albright, J., & Urban, N. M. (2021). Differentiable programming for online training of a neural artificial viscosity function within a staggered grid Lagrangian hydrodynamics scheme. Machine Learning: Science and Technology, 2, 025015. doi:10.1088/2632-2153/abd644

Mousa, M. M., & Ma, W.-X. (2020). Efficient modeling of shallow water equations using the method of lines and artificial viscosity. Modern Physics Letters B, 34, 2050051. doi:10.1142/S0217984920500517

Neumann, J. V., & Richtmyer, R. D. (1950). A method for the numerical calculation of hydro-dynamic shocks. Journal of applied physics, 21, 232–237. doi:10.1063/1.1699639

Nuttall, J. G., O'leary, G. J., Panozzo, J. F., Walker, C. K., Barlow, K. M., & Fitzgerald, G. J. (2017). Models of grain quality in wheat—A review. Field Crops Research, 202, 136–145. doi:10.1016/j.fcr.2015.12.011

Oberkampf, W. L., & Blottner, F. G. (1998). Issues in Computational Fluid Dynamics Code Verification and Validation. AIAA Journal, 36, 687-695. doi:10.2514/2.456

Oliveira, F., Khatchatourian, O. A., & Bilhain, A. (2007). Thermal state of stored products in storage bins with aeration system: experimental-theoretical study. Engenharia Agrícola, 27, 247–258.

Panigrahi, S. S.; Singh, C. B.; Fielke, J.; Zare, D. (2020). Modeling of heat and mass transfer within the grain storage ecosystem using numerical methods: A review. Drying Technology, Taylor & Francis, v. 38, n. 13, p. 1677–1697.

Rigoni, D., Pinto, M. A., & Kwiatkowski Jr., J. E. (2021). Comparison among numerical approximations in the simulation of the grain mass aeration process. Proceedings of the XLII Ibero-Latin-American Congress on Computational Methods in Engineering and III Pan-American Congress on Computational Mechanics, ABMEC-IACM.

Rigoni, D., Pinto, M. A., & Kwiatkowski Jr., J. E. (2022). Verification and error analysis for the simulation of the grain mass aeration process using the method of manufactured solutions. Biosystems Engineering, 223(1), 149-160. doi:https://doi.org/10.1016/j.biosystemseng.2022.08.006

Roy, C. J. (2005). Review of code and solution verification procedures for computational simulation. Journal of Computational Physics, 205, 131-156. doi:10.1016/j.jcp.2004.10.036

Tannehill, J. C., Anderson, D. A., & Pletcher, R. H. (1997). Computational Fluid Mechanics and Heat Transfer (Vol. 2).

Thomas, L. H. (1949). Elliptic problems in linear difference equations over a network. Watson Sci. Comput. Lab. Rept., Columbia University, New York, 1, 71.

Thorpe, G. R. (2001). Physical basic of aeration. In: S. Navarro, R. T. Noyes, The Mechanics and Physics of Modern Grain Aeration Management, 1, 125-185.

Van Genuchten, M. T., Service, U. S., & Alves, W. J. (1982). Analytical Solutions of the One-dimensional Convective-dispersive Solute Transport Equation. U.S. Department of Agri-culture, Agricultural Research Service.

Xuana, G., Zheng, H., Xiaoyu, S., & others. (2017). A Two-dimensional lattice Boltzmann method for compressible flows. Acta Informatica Malaysia (AIM), 1, 32–35.

9. RESPONSIBILITY NOTICE

The authors are the only responsible for the printed material included in this paper.